VOL. 7, NO. 9, SEPTEMBER 2012 ISSN 1819-6608
ARPN Journal of Engineering and Applied Sciences


www.arpnjournals.com

TIME-DEPENDENT BEHAVIOR OF PILE UNDER LATERAL LOAD USING THE BOUNDING SURFACE MODEL

Qassun S. Mohammed Shafiqu and Maarib M. Ahmed Al-Sammaraey
Department of Civil Engineering, Nahrain University, Iraq
E-Mail: qassun@yahoo.com

ABSTRACT

Time-dependent behavior of pile embedded in saturated porous medium has been investigated in this study using the finite element method. This behavior occurs due to consolidation of the saturated medium which was implemented through a fully coupled Biot formulation. The finite element analyses were carried out using the elasto-plastic bounding surface model for representing soil surrounding the pile. The model together with Biot consolidation were implemented and verified. The investigation of the time-dependent behavior of pile under lateral load was then carried out in five types of cohesive soils and the results showed that the elasto-plastic bounding surface model provide a realistic stress distribution within the soil mass around the pile. Also, it was observed that significant influence of time (i.e., consolidation process) on pile displacements will appeared. Finally, the study shows a significant influence of the critical state parameters λ and κ on the time-dependent behavior of pile under lateral load.

Keywords: pile, finite element, bounding surface model, consolidation, lateral response.

INTRODUCTION

Pile foundations are usually used when heavy structural loads have to be transmitted through weaker subsoil. When used under tall chimneys, high rise structures and coastal and offshore structures, piles are also subjected to significant amounts of lateral loads and overturning moments besides axial loads. Thus proper attention has to be given in designing such pile-supported structures under lateral loads. In very soft clayed ground, however, even if the bearing capacity of a pile foundation is sufficient enough to resist vertical load, the long-term settlement of the pile foundation due to vertical static load cannot be neglected. Sometimes this causes big problems, especially in those structures like railway bridges whose deformation is strictly restricted. For performance based design, it is necessary to check the vertical displacement not only in short-term, but also in long-term. Many prediction methods can be found in literature for the settlement in soft ground. But for pile foundation, due to the difficulty in evaluating the interaction of pile-soil-pile system, quantitative prediction method for long-term settlement in soft ground is still need to be developed.

With the development of the finite element method, the ability to numerically model complicated soil structure has become possible. Geotechnical construction is one such area that has been investigated extensively by the finite element method. The work presented in this study is concerned with one particular area of geotechnical construction, that of piles. However, to be successfully used in practical design, the soil model should be able to represent the soil behavior as close to reality and can be calibrated by conventional field or lab testing. On the other hand, the model should be able to realistically capture the most important aspects of soil-structure nonlinearities.

In view of this, the present paper focuses on the study of time-dependent behavior of piles in saturated cohesive soils subjected to lateral loads through 2D finite-element analyses.

BOUNDING SURFACE MODEL FOR SOIL

The numerical implementation of the model and the parameters associated with the model are available in Dafalias and Herrmann, (1986) and Herrmann *et al*., (1987). The elasto-plastic rate relations are the total strain rate is consisting of two parts: elastic strain and plastic strain.

$$\dot{\varepsilon}_{ij} = \dot{\varepsilon}_{ij}^{e} + \dot{\varepsilon}_{ij}^{p} \tag{1}$$

where a dot indicates a rate and an associated flow rule is assumed. The inverse form of the constitutive relations is obtained as:

$$\dot{\sigma}_{ij} = D_{ijkl}\,\dot{\varepsilon}_{kl} \tag{2}$$

$$D_{ijkl} = G\left(\delta_{ki}\delta_{lj} + \delta_{kj}\delta_{li}\right) + \left(K - \frac{2}{3}G\right)\delta_{ij}\delta_{kl}$$

$$-\frac{\bar{h}(L)}{g}\left[3KF_{,f}\delta_{ij} + \frac{G}{J}F_{,f}s_{ij} + \frac{\sqrt{3}G}{\cos(3\alpha)}\frac{F_{,\alpha}}{bJ}\left(\frac{s_{in}s_{nj}}{J^2} - \frac{3S^3 s_{ij}}{2J^4} - \frac{2\delta_{ij}}{3}\right)\right]$$

$$\left[3KF_{,f}\delta_{kl} + \frac{G}{J}F_{,f}s_{kl} + \frac{\sqrt{3}G}{\cos(3\alpha)}\frac{F_{,\alpha}}{bJ}\left(\frac{s_{kn}s_{nl}}{J^2} - \frac{3S^3 s_{kl}}{2J^4} - \frac{2\delta_{kl}}{3}\right)\right] \tag{3}$$

where

$$L = \frac{1}{g}\left\{3KF_{,f}\dot{\varepsilon}_{kk} + \frac{G}{J}F_{,f}s_{ij}\dot{\varepsilon}_{ij} + \frac{\sqrt{3}G}{\cos(3\alpha)}\frac{F_{,\alpha}}{bJ}\left[\left(\frac{s_{ik}s_{kj}}{J^2} - \frac{3S^3 s_{ij}}{2J^4}\right)\dot{\varepsilon}_{ij} - \frac{2\dot{\varepsilon}_{kk}}{3}\right]\right\} \tag{4a}$$

$$B = K_p + 9K(F_{,I})^2 + G\left(F_{,I}\right)^2 + G\left(\frac{F_{,\alpha}}{bJ}\right)^2 \quad (4b)$$

and where K and G represent the elastic bulk and shear moduli, respectively; δ_{ij} is the Kronecker delta; K_p the plastic modulus; I , J and α are the stress invariants; $1 \leq b \leq \infty$ and F represents the analytical expression of the bounding surface; s_{ij} represents the deviatoric part of the stress tensor and $S^3 = (s_{ij}s_{jk}s_{ki})/3$ represents the third deviatoric stress invariant.

FORMS OF THE BOUNDING SURFACE

The analytical definition of the bounding surface may assume many particular forms provided it satisfies certain requirements concerning the shape of the surface (Dafalias and Herrmann, 1986). The analytical expressions for a composite form of the bounding surface, consisting of two ellipses and one hyperbola, with continuous tangents at their connecting points (Figure-1), are presented below (Dafalias and Herrmann, 1986).

For ellipse 1:

$$F = (\bar{I} - I_o)\left(\bar{I} + \frac{R-2}{R}I_o\right) + (R-1)^2\left(\frac{J}{N}\right)^2 = 0 \quad (5)$$

For the hyperbola:

$$F \equiv \left(\bar{I} - \frac{I_o}{R}\right)^2 - \left(\frac{J}{N} - \frac{I_o}{R}\right)\left[\frac{J}{N} - \frac{I_o}{R}\left(1 + 2\frac{RA}{N}\right)\right] = 0 \quad (6)$$

For ellipse 2:

$$F = (\bar{I} - TI_o)[\bar{I} - (T + 2\xi)I_o] + \rho\bar{J}^2 = 0 \quad (7a)$$

where: $\xi = -\frac{T(Z+TF')}{Z+2TF'}$, $\rho = \frac{T^2}{Z(Z+TF')}$ (7b)

$$F' = \frac{N}{\sqrt{1+y^2}}, \quad y = \frac{RA}{N}, \quad Z = \frac{N}{R}\left(1 + y - \sqrt{1+y^2}\right) \quad (7c)$$

ELASTO-PLASTIC BOUNDING SURFACE MODEL PARAMETERS

The parameters are divided into the following three groups (Kaliakin, 2005):

Traditional material constants

λ = slope of consolidation line
κ = slope of swelling line
N (α) = slope of critical state line, Nc = N in compression Ne =N in extension
υ= Poisson's ratio

Surface configuration parameters

R(α) = R > 1defines the point I1 =I◦/R (Figure-1), which together with point J1 defines the coordinates of point H which is the intersection of F = 0 and CSL, Rc = R in compression, Re = R in extension, shape parameter determine the ratio of the major to minor axis of ellipse 1 (2.0 ≤ R ≤ 3.0).

A (α) = parameter defines the distance D = AI◦ of apex H of the hyperbola from its center G intersection of the two asymptotes and thus pertains only to the composite form of the surface, Ac = A in compression, Ae = A in extension, shape parameter controls the shape of the hyperbolic portion of the bounding surface (0.02 ≤ A ≤ 0.2).

T = It /I◦ parameter which determines the purely tensile strength of the material, and T also pertains to the composite form of the surface, C = 0 ≤ C <1 parameter which determines the center of the bounding surface Ic = CI◦. The projection center parameter (0 ≤ C ≤ 1) defines the point along the I-axis which serves as the projection center in the radial mapping rule.

Hardening parameters

s_p = parameter which determines indirectly "elastic nucleus". For s_p = 1 the elastic nucleus degenerates to point Ic center of bounding surface and as $s_p \rightarrow \infty$ the elastic nucleus expands towards the bounding surface.

h = slope-hardening factor, which is a function of lode angle (α), hc = for compression (hc = h (π/6)), he = for extension (he = h (¯π/6)) a and w = hardening parameters if the single ellipse version of the bounding surface is used.

m = a positive model parameter.

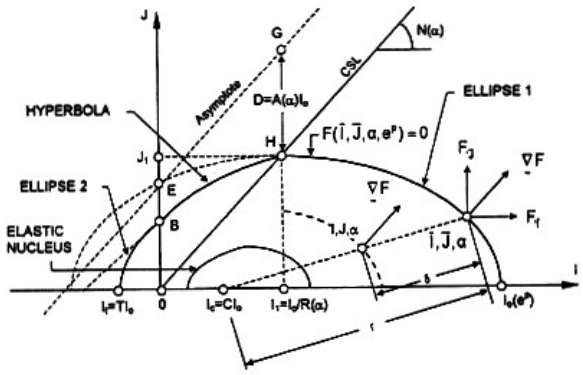

Figure-1. Bounding surface in stress invariants space (after Dafalias and Herrmann, 1986).

FINITE ELEMENT FORMULATION

The elasto-plastic bounding surface model described above is incorporated in a finite element program, which has the feature of modeling two-dimensional (plane strain and axisymmetric) geotechnical problems such as consolidation, written by FORTRAN90 language. This program is primarily based on the programs presented by Smith and Griffiths (2004) for the analysis of two-dimensional solid by finite element method utilizing elastic constitutive relationship and which is modified for the purpose of this study. So in addition to the elasto-plastic bounding surface model, the

program allows one to assign linear elastic behavior to any part of the problem geometry together with Mohr-Coulomb model for representing cohesionless soil. Description of all of the program features is beyond the scope of this paper, and a brief summary of the feature relevant to this study is given below.

Transient formulation

In the case of a pile in saturated porous medium, the loading is time-dependent, so an incremental formulation was used in the following work producing the matrix version of the Biot equation at the element level presented below (Lewis and Schrefler, 1987).

$$\begin{bmatrix} K & L \\ L^T & S+\bar{\alpha}H\Delta t_k \end{bmatrix}\begin{Bmatrix} \bar{u} \\ \bar{p} \end{Bmatrix} = \begin{bmatrix} K & L \\ L^T & S-(1-\bar{\alpha})H\Delta t_k \end{bmatrix}\begin{Bmatrix} \bar{u} \\ \bar{p} \end{Bmatrix} + \begin{Bmatrix} dF/dt+C \\ \bar{F} \end{Bmatrix} \quad (8)$$

where: K = element solid stiffness matrix, L = element coupling matrix, H = element fluid stiffness matrix, $\bar{u}$ = change in nodal displacements, $\bar{p}$ = change in nodal excess pore-pressures, S = the compressibility matrix, $\bar{F}$ = load vector, Δt = calculation time step, $\bar{\alpha}$ = time stepping parameter (=1 in this work), dF/dt = change in nodal forces.

TIME-DEPENDENT BEHAVIOR OF PILE IN SEVERAL TYPES OF COHESIVE SOIL UNDER LATERAL LOADING

A time-dependent behavior of a pile with diameter Dp = 1m and length of 10m which can be considered to be short pile embedded in a layer of saturated elasto-plastic cohesive soil which obeys the bounding surface model is studied. This problem was previously investigated by Carter and Taibat (2001) but the pile was embedded in a layer of saturated cohesionless soil which obeys the Mohr-Coulomb failure criterion where the friction angle of the soil is assumed to be φ = 30° and the soil is also assumed to have a submerged unit weight of $\gamma_{sub} = 0.7\ \gamma_w$, where γ_w is the unit weight of pore water, a Young's modulus for fully drained conditions given by E's = 3000 γ_w and a Poisson's ratio v' = 0.30. The predicted load-displacement curves for the pile head, for cases where the pile deforms under undrained and drained conditions are presented in Figures (3) and (4), respectively. The figures show good comparisons between the results of the program modified for the purpose of this study and those obtained by Carter and Taibat (2001).

In this study five types of cohesive soils are considered in the analysis, which are Kaolin mix soil (K2-soil), Kaolin soil (K1-soil), Marine silty soil (M-soil), Grenoble soil (G-soil) and Umeda soil (U-soil); the parameters of these soils are presented in Table-1 (Kaliakin and Dafalias, 1991), where the parameters sp, a and w are fixed for all type of soils as 1, 1.2 and 5 respectively. The pile is subjected to a lateral loading applied at the midline.

The problem is analyzed assuming elastic model for pile material with parameters given in Table-2, and elasto-plastic bounding surface model for soil surrounding the pile. The finite element mesh and dimensions of the problem are shown in Figure-2. All elasto-plastic analyses have been carried out using 8-nodes quadrilateral finite element.

In order to examine the time dependent consolidation behavior of the pile, it is convenient to introduce a non-dimensional time factor T_v, defined as:

$$T_v = \frac{k(1-\nu_s')E_s't}{\gamma_w(1-2\nu_s')(1+\nu_s')D_p^2} \quad (9)$$

Where

k is the coefficient of soil permeability and t represents time.

Table-1. Bounding surface parameters for the five cohesive soils (after Kaliakin and Dafalias, 1991).

Properties / soil type	λ	κ	ν	M_c	M_e	R_c	R_e	A_c	A_e	C	h_c	h_e
Kaolin mix	0.075	0.011	0.22	1.35	0.9	3.05	1.71	0.18	0.15	0.49	11	9.6
Kaolin	0.14	0.05	0.2	1.05	0.85	2.65	2.25	0.02	___[a]	0.7	4	5.6
Marine silty	0.178	0.052	0.2	1.07	0.79	2.2	___[a]	0.1	___[a]	0.4	10	10
Grenoble	0.2	0.1	0.15	0.78	0.8	2.5	2	0.02	0.02	0.5	4.3	4.3
Umeda	0.343	0.105	0.15	0.77	0.61	2.39	___[a]	0.01	___[a]	0.2	2	___[a]

[a] Material response in extension was not simulated

Table-2. Properties for pile material (after Carter and Taibat, 2001).

Properties	Values
γ_c, unit weight, kN/m^3	24.0
Poisson's ratio	0.2
E_p, modulus of elasticity, kN/m^2	30*10^6

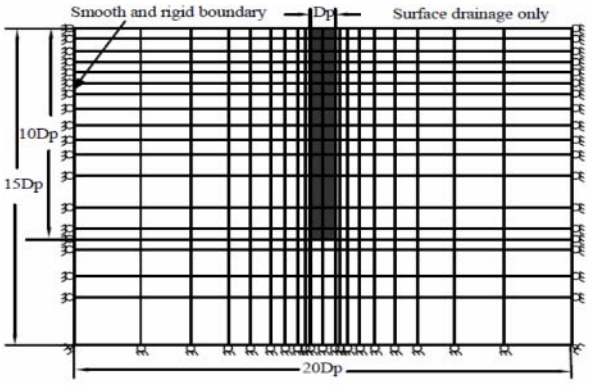

Figure-2. Finite element mesh.

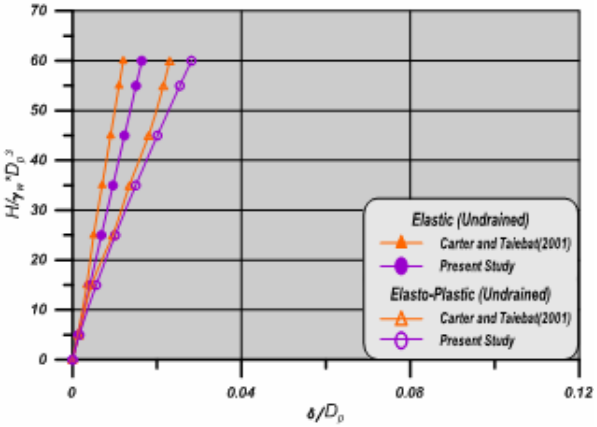

Figure-3. Comparison of the pile response with different soil models, each deforming under undrained conditions.

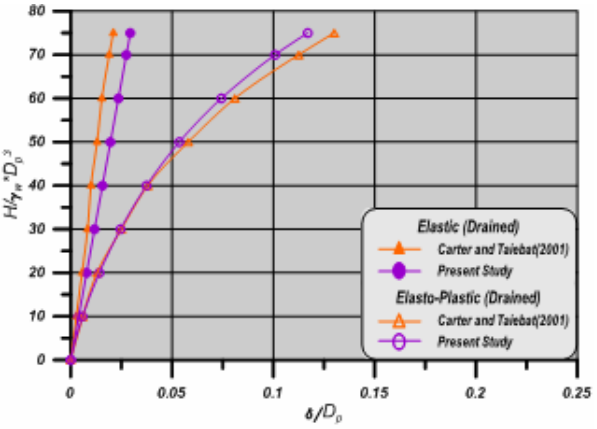

Figure-4. Comparison of the pile response with different soil models, each deforming under fully drained conditions.

In the elasto-plastic analysis, the lateral pile displacements developed depending on lateral loads H = $5\gamma_w \times D_p^3$, H = $35\gamma_w \times D_p^3$ and H = $60\gamma_w \times D_p^3$ and time factors T_v = 0.0001, 0.1 and 1.0 along depth of pile embedded in K2-soil, K1-soil, M-soil, G-soil and U-soil are shown in Figures (5a, 5b, 5c, 5d and 5e, respectively). It can be observed that the maximum displacement appeared at the head of pile decreasing with the depth and the lower lateral loading the lower are the lateral displacements along the depth of pile, also there appear to be significant influence of time (i.e., consolidation process) on the displacements. The influence become more clearly with increasing the lateral loading that higher displacements were observed with time due to consolidation process, and this appear obviously in Figures (6a, 6b, 6c, 6d and 6e) which draws the lateral time-dependent displacements of pile head under lateral loadings H= 5, 15, 25, 35, 45, 55 and $60(\gamma_w \times D_p^3)$ in all soils. Also from these Figures a reduction in displacements by about 90% and 40% are observed if about 10% and 60% of maximum lateral load is applied, respectively. And it can be indicated that the displacement of pile head in all cohesive soils under all loadings will increased during consolidation process by about 23% to 53% of that at the beginning time of consolidation (i.e., T_v = 0.0001) due to dissipation of excess pore water pressure according to the manner discussed below, which causes higher effective stress and thus higher displacements. The enlargement of displacement will be in a decreasing rate ranging between about 14% to 35% at earlier stage of consolidation process from time factor T_v = 0.0001 to 0.01 being between 7% to 18% at the later stage of consolidation from T_v = 0.01 to 1.0.

The excess pore water pressure (EPWP in kPa) contours at lateral load of H = $60\gamma_w \times D_p^3$ with time factors T_v = 0.0001, 0.1 and 1.0 for K2-soil are shown in Figures (7a, 7b and 7c), for K1-soil in Figures (8a, 8b and 8c), for M-soil in Figures (9a, 9b and 9c), for G-soil in Figures (10a, 10b and 10c) and for U-soil in Figures (11a, 11b and 11c). In these figures it should be observed that all of pore pressures are positive in front of pile with the direction of loading reflecting the compression due to lateral loading on pile head and negative at back side of pile due to unloading and they are concentrated near the upper part of pile. And it can be noticed that the EPWP distribution is irregular at the beginning time of consolidation T_v= 0.0001 became more regular with time, also the long term dissipation will be in higher rate near the head of the pile. At time factor T_v =1.0 the EPWP values near head of pile will be lower than that near the base being increased away from piles and remains zero below it.

With regard to the influence of bounding surface parameters on the lateral displacement of pile under lateral loading and from Figure-12 which plot the largest lateral displacements of pile with depth for the five types of cohesive soils under the higher lateral loading H = $60\gamma_w \times D_p^3$ and time factor T_v = 1.0 it can be concluded that the lateral displacement increase with increasing the values of the model parameters **λ** and **ν** that for cohesive soils that have higher values of the parameters **λ** and **ν** and lower values of M, **ν**, R, h, A, and C larger displacements were noticed especially at the pile head. Also lower rate of increasing the displacements with time were noticed for K2-soil which have smaller values of the parameters **λ**

and **κ** and larger values for other parameters being higher in the soils with larger values of **λ** and **κ** parameters and lower values for the others.

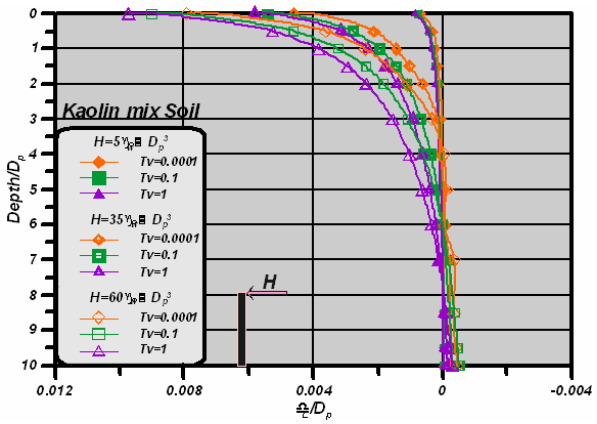

Figure-5(a). Lateral displacement of pile with depth (K2-soil).

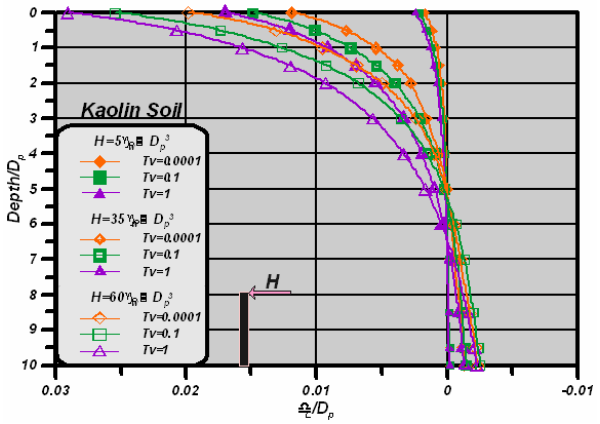

Figure-5(b). Lateral displacement of pile with depth (K1-soil).

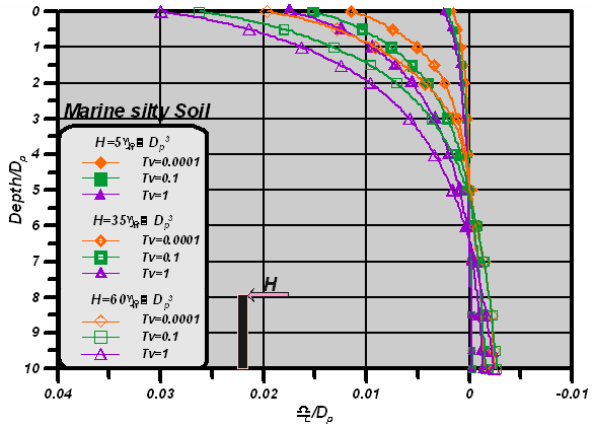

Figure-5(c). Lateral displacement of pile with depth (M-soil).

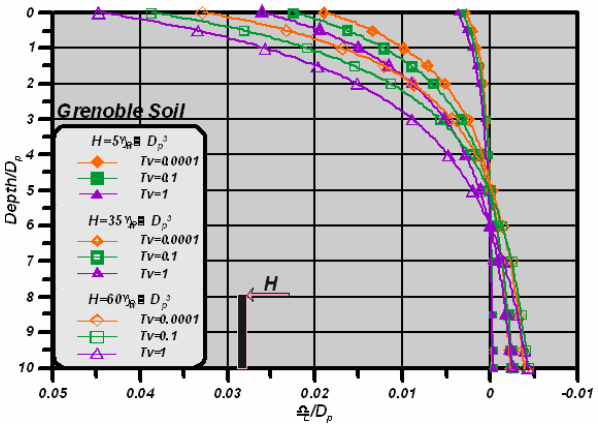

Figure-5(d). Lateral displacement of pile with depth (G-soil).

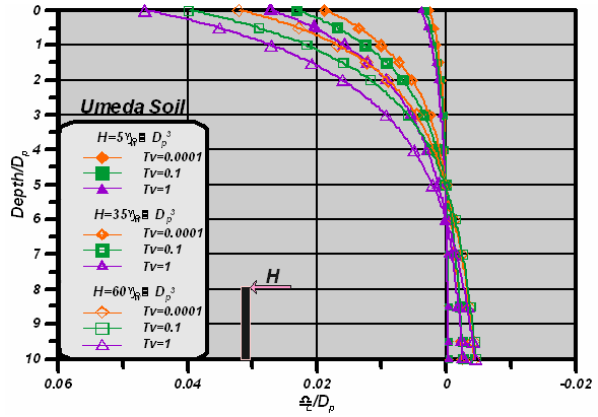

Figure-5(e). Lateral displacement of pile with depth (U-soil).

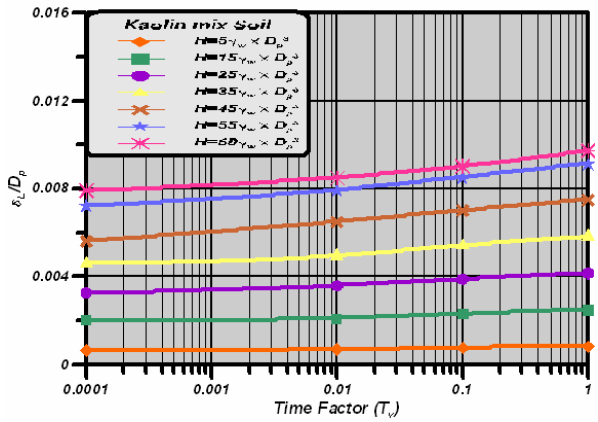

Figure-6(a). The time-dependent lateral displacements of the pile head (K2-soil).

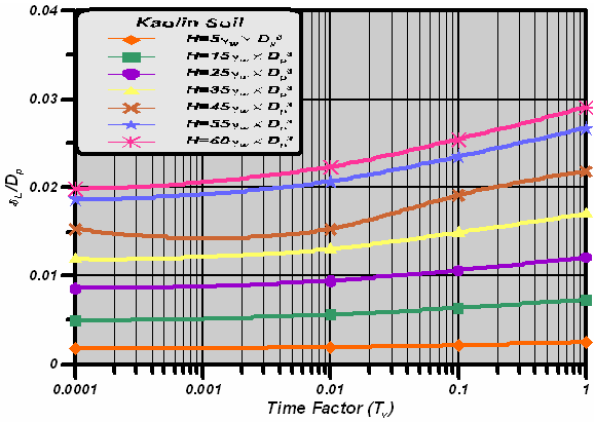

Figure-6(b). The time-dependent lateral displacements of the pile head (K1-soil).

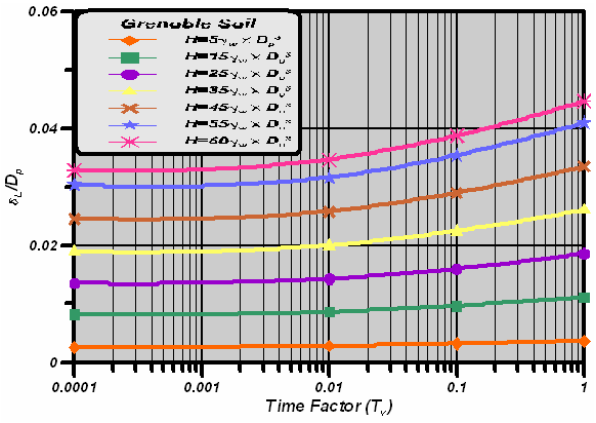

Figure-6(d). The time-dependent lateral displacements of the pile head (G-soil).

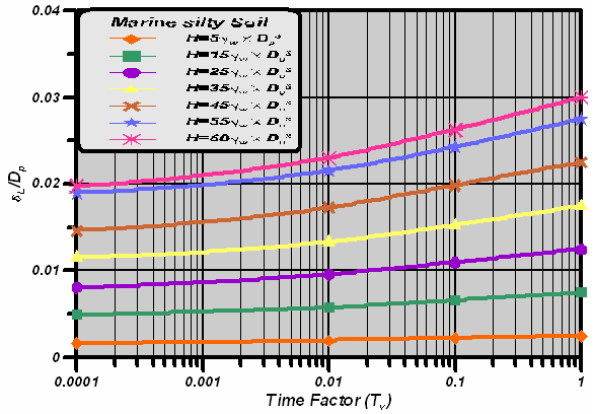

Figure-6(c). The time-dependent lateral displacements of the pile head (M-soil).

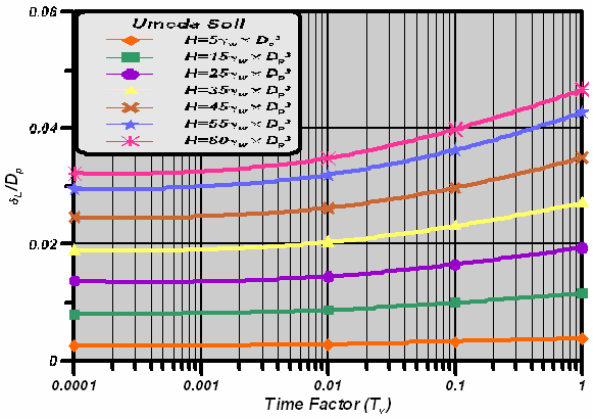

Figure-6(e). The time-dependent lateral displacements of the pile head (U-soil).

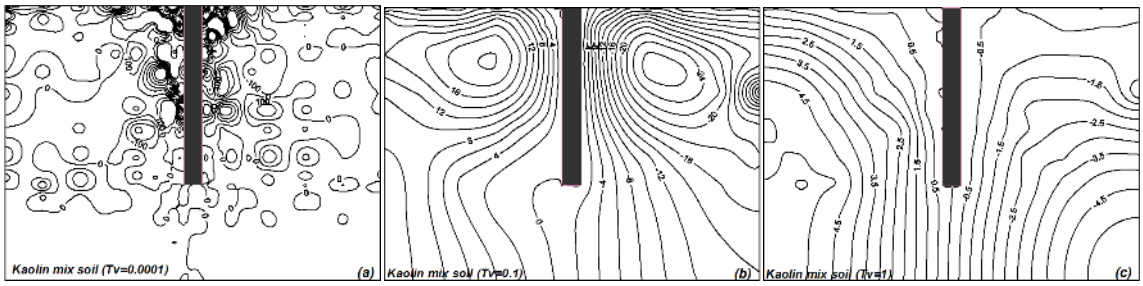

Figure-7. EPWP for pile under lateral loading in K2-soil.

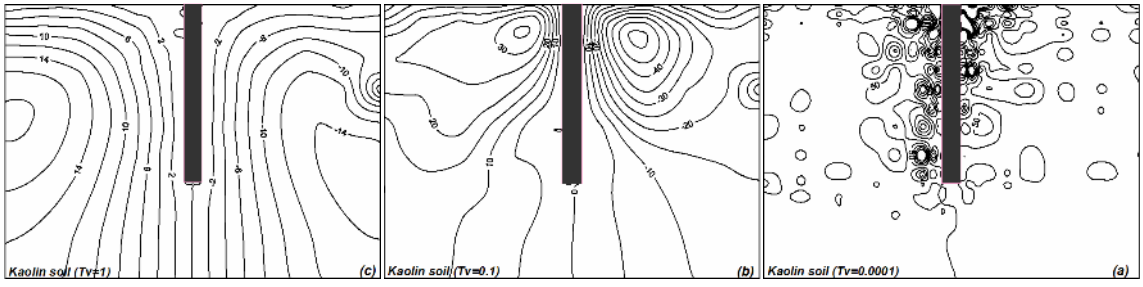

Figure-8. EPWP for pile under lateral loading in K1-soil.

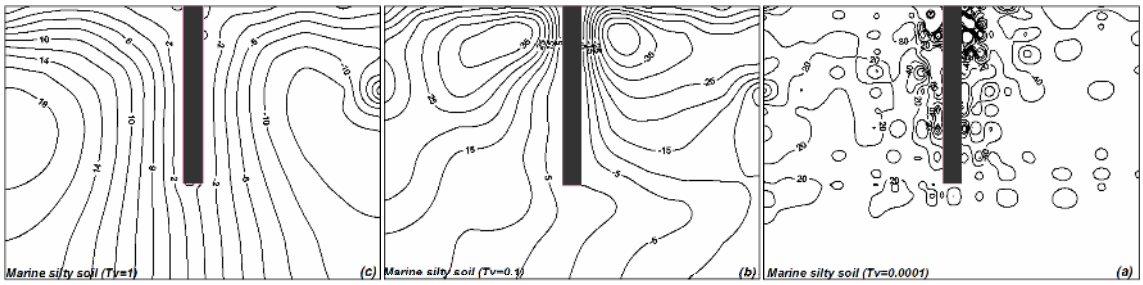

Figure-9. EPWP for pile under lateral loading in M-soil.

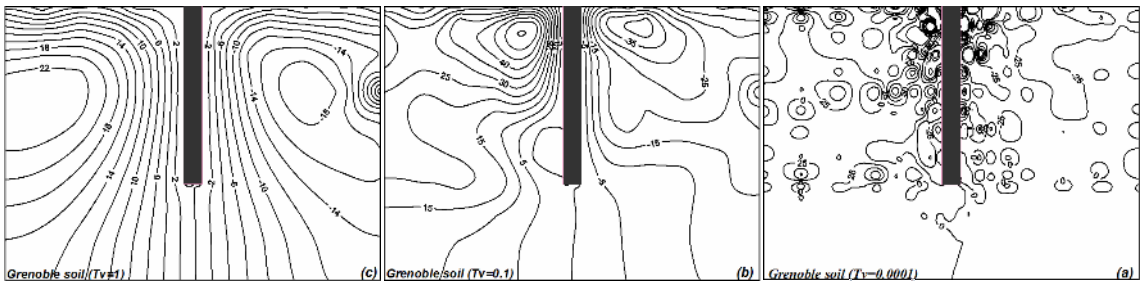

Figure-10. EPWP for pile under lateral loading in G-soil.

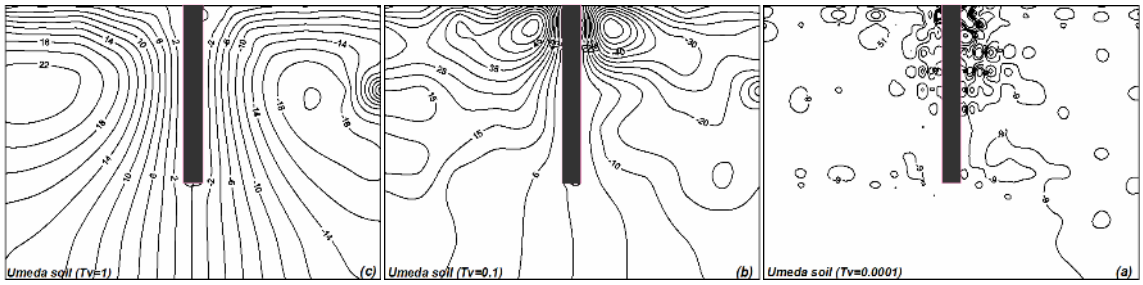

Figure-11. EPWP for pile under lateral loading in U-soil.

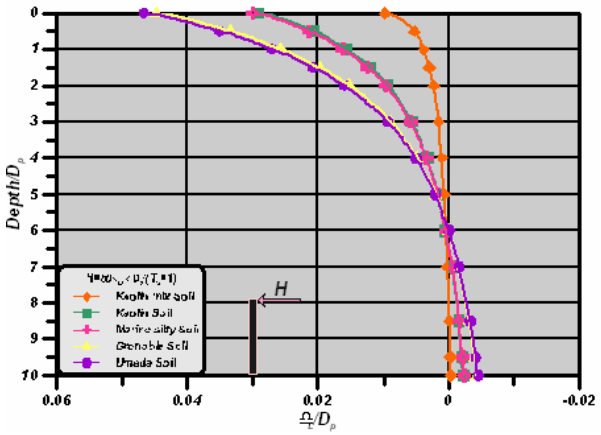

Figure-12. Lateral displacement of pile with depth (All Soils).

CONCLUSIONS

A finite element analysis of the time-dependent behavior of pile in saturated cohesive soils subjected to lateral loadings. The nonlinear stress-strain behaviors of soils are modeled via bounding surface type plasticity, which allows the plastic displacement to occur for stress points within the surface. A parametric study is carried out to address the influence of various factors, such as load intensity, consolidation process and bounding surface parameters on the prediction of time-dependent piled foundation behavior in several types of cohesive soils and the following conclusions can be drawn:

- For pile subjected to lateral load the long term lateral displacement of pile head in all cohesive soils under all loadings may reach to about 50% of that from short term due to dissipation of excess pore water pressure.
- There appear to be significant influence of time (i.e., consolidation process) on the displacements, thus for piles in saturated clays it is highly recommended to take such influence in to consideration by the designer.
- For cohesive soils that have higher values of the bounding surface model parameters **λ** and **κ** and lower values of M, **ν**, R, h, A, and **C**, lower excess pore

pressure contours exist. This causes higher effective stress and thus higher lateral displacements.

- The EPWP distribution is irregular at the beginning time of consolidation became more regular with time; also the long term dissipation will be in higher rate near the head of the pile. With time the EPWP values near head of pile will be lower than that near the base being increased away from piles and remains zero below it.

REFERENCES

Dafalias Y. F. and Herrmann L. R. 1986. Bounding Surface Plasticity II: Application to Isotropic Cohesive Soils. Journal of Engineering Mechanics, ASCE. 112(12): 1263-1291.

Herrmann L. R., Kaliakin V. N., Shen C. K., Mish K. D. and Zhu Z. 1987. Numerical Implementation of Plasticity Model for Cohesive Soils. Journal of Engineering Mechanics. 113(4): 500-519.

Kaliakin V. N. and Dafalias Y. F. 1991. Details Regarding the Cohesive Soils. Civil Engineering Report No.91-1, University of Delaware, Newark.

Kaliakin V.N. 2005. Parameter Estimation for Time-Dependent Bounding Surface Models. Geo-Frontiers Conference; Soil Constitutive Models: Evaluation, Selection, and Calibration. Geotechnical special publication. (128): 237-256.

Lewis R. W. and Schrefler B. A. 1987. The Finite Element Method in the Deformation and Consolidation of Porous Media. John Wiley and Sons, Ltd., London, U.K.

Smith I. M. and Griffiths D. V. 2004. Programming Finite Element Method. 4th Ed. John Wiley and Sons.

Carter J.P. and Taiebat H.T. 2001. A semi-analytical finite element method for three dimensional consolidation analysis. Civil Engineering Department, the University of Sydney, Sydney, NSW 2006, Australia, Computers and Geotechnics. pp. 55-78.